Anomalous integer quantum Hall states in coupled double quantum wells and the effect of Landau level broadening



1999 J. Phys.: Condens. Matter 11 3711

(http://iopscience.iop.org/0953-8984/11/18/307)

J. Phys.: Condens. Matter **11** (1999) 3711–3728. Printed in the UK PII: S0953-8984(99)01253-9

# Anomalous integer quantum Hall states in coupled double quantum wells and the effect of Landau level broadening

I S Millard†, N K Patel‡, C L Foden‡, A R Hamilton†, M Y Simmons†, D A Ritchie†, G A C Jones† and M Pepper†‡

† Cavendish Laboratory, University of Cambridge, Madingley Road, Cambridge CB3 0HE, UK
‡ Toshiba Cambridge Research Centre, 260, Science Park, Milton Road, Cambridge CB4 4WE, UK

Received 26 January 1999

**Abstract.** In this paper, we discuss the effect of a strong perpendicular magnetic field component upon a range of coupled double quantum well (CDQW) devices. With increasing inter-layer tunnelling, we observe a transition from double- to single-layer characteristics in the magneto-transport data. The effect of the perpendicular field upon a CDQW has also been considered through a self-consistent Poisson/single-particle Schrödinger model. The implications of the experimental and theoretical results for the current analysis of the transport properties of CDQWs are discussed.

## 1. Introduction

In order to describe the transport properties of a CDQW it is necessary to detail their general characteristics in a perpendicular field. Therefore, the introduction is subdivided into three sections. Firstly, the effect of a perpendicular magnetic field upon the transport characteristics of DQWs is briefly introduced. Secondly, a short description of the absence of odd QH states in CDQWs at resonance due to many-body effects is given. Thirdly, we have a note upon the importance of analysing CDQWs together with a self-consistent model.

### *1.1. Formation of LLs in DQWs*

Consider initially an uncoupled DQW in a perpendicular magnetic field. In the absence of inter-layer tunnelling ($\Delta_{SAS} \rightarrow 0$) the 2DEGs are fully localized within their respective QWs. As a result, Landau levels in each 2DEG (QW) are populated independently of one another. Upon sweeping a perpendicular magnetic field, the longitudinal resistance of each of the layers oscillates due to Shubnikov–de Haas (SdH) oscillations arising from the depopulation of LLs in each layer. As the two layers are independent, a fast Fourier transform of these oscillations away from resonance reveals two frequencies, reflecting two, different 2DEG densities, $N_{top}$ and $N_{bottom}$. At resonance the two 2DEGs have equal densities and one resolves a FFT frequency in the SdH oscillations corresponding to half of the total carrier density: only even filling indices ($\nu_{total} = 2, 4, 6, \ldots$) are observed in the SdH data, where $\nu_{total} = N_{total}h/eB_{\perp}$ and $N_{total} = N_{top} + N_{bottom}$. Experimental magneto-transport characteristics of an uncoupled DQW are illustrated in section 2.1.

As the two QWs are brought into close proximity, the first ground state associated with each of the QWs hybridizes, the degree of hybridization being determined by the overlap

0953-8984/99/183711+18$19.50  

of the two wavefunctions. By matching the densities in each QW the inter-layer tunnelling is maximized (resonance) and a symmetric and anti-symmetric subband are formed with an energy separation $\Delta_{SAS}$. Upon applying a perpendicular magnetic field one must now consider, in addition to the Zeeman ($g^*\mu_B B$) and cyclotron ($\hbar\omega_c$) energies, the gap arising from the inter-layer tunnelling.

For all CDQW densities, both on and off resonance, the resistance minima in the SdH oscillations should correspond to the occupation of LLs in either of the two subbands. In this respect the CDQW should be similar to two uncoupled 2DEGs. A significant difference between the CDQW and the uncoupled 2DEGs should arise as both systems are brought onto resonance. In the CDQW, the degeneracy of the subbands has been lifted by wavefunction hybridization; therefore the two subbands have different carrier densities. One should see the manifestation of the two, differing, densities as a convolution of two FFT frequencies in the SdH data, in contrast to the single FFT frequency in the uncoupled case.

However, it is observed experimentally that upon applying a *high* magnetic field to the CDQW, at resonance, one does *not* see the two FFT frequences. Rather, the system forms strong even and odd filling indices ($\nu_{total}$) associated with the *total* carrier density. As will be discussed further in later sections, this is a result of the charge associated with the two subbands occupying the same physical space because their wavefunctions are delocalized across the DQW. As such, it is incorrect to regard the two subbands as being independent of one another and the CDQW behaves as if it were a single 2DEG [1, 2, 12]. The magnetic field thus causes a transition from bilayer characteristics at low magnetic fields to single layer behaviour at high fields.

### *1.2. Absence of odd QH states*

A number of experimental studies [3–8] utilizing samples with differing degrees of tunnelling and carrier densities have shown that the odd $\nu_{total}$ IQH states seen in CDQWs may be destroyed at a critical perpendicular field and tunnelling energy.

MacDonald *et al* [9] have proposed that the origin of these missing states lies in a competition between the inter-layer coupling and the intra-layer e–e Coulomb energy, the result of which is a 'bi-layer phase transition'.

The mechanism [4, 9] proposed for the destruction of the odd IQH states, using the $\nu = 1$ state as an example, is outlined as follows. In order for this theory to be applicable to a CDQW at resonance, the spin split LLs must be fully resolved and the tunnelling coupling energy be the smallest energy scale ($\hbar w_c \gg g^*\mu_B B > \Delta_{SAS}$): figure 1 illustrates the energies of the first two LLs in each subband as a function of magnetic field.

All of the odd IQH states ($\nu = 1, 3, 5, \ldots$) seen in this limit are a product of the tunnelling gap $\Delta_{SAS}$ [4] and upon applying a large perpendicular field, the anti-symmetric subband can be depopulated. One then sees a $\nu = 1$ state in which all of the charge occupies the symmetric subband [4, 9]. The absence of this QH state would then suggest that a new ground state has been formed in which the single particle tunnelling gap ($\Delta_{SAS}$) has been suppressed. Likewise, the suppression of other odd QH states would also imply the loss of the $\Delta_{SAS}$ gap.

In the theory [9]†, two configurations of the electron distribution are considered: either the formation of the symmetric and anti-symmetric subbands with a delocalized charge distribution, or the localization of charge in both the QWs due to many-body effects.

Whereas the first configuration generates odd QH states, the second leads to the suppression of odd QH states. Theoretical calculations have shown that the strength of the

† What follows is a approximate description; interested readers are referred to the original papers for a more detailed description.

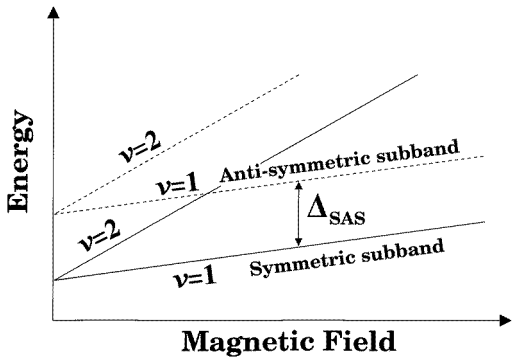


**Figure 1.** First two spin split LLs from each subband in a CDQW.

intra-layer Coulomb interactions determines whether it is favourable to form the delocalized charge distribution or to localize the charge in the QWs. The latter state becomes more favourable in 2DEGs with a large Coulomb interaction energy.

As an applied magnetic field acts to localize the electrons, the e–e interactions become increasingly important. Therefore a CDQW at resonance should be driven through a transition from a symmetric charge distribution (stabilized through inter-layer tunnelling) to two correlated layers with no charge excitation gap as the field is increased: this transition destroys the tunnelling gap and suppresses the odd $\nu = 1$ QH state. The suppression of this and other odd IQH states has been studied in both single, wide QWs (SWQWs) [5] and CDQW hetero-structures [4], the observations seeming to agree with the 'coupled' to 'bi-layer' (suppressed tunnelling) transition.

An additional phase transition has then been proposed for the $\nu = 1$ QH states. In this transition a continuous evolution of the QH state to the formation of a many-body correlated $\psi_{111}$ state is predicted [7]. The following work discusses the first of these transitions; the transition to a $\psi_{111}$ state is not considered within the range of experimental parameters dealt with.

### *1.3. Self-consistent models*

There are, however, some noticeable features in a CDQW's magneto-transport data that require an explanation. In particular, both the $\nu = 1$ [1, 10, 11] and $\nu = 2$ [1] QH states have been observed to remain whilst the subband densities are mismatched from resonance.

Studies utilizing single [13], single wide [14], parabolic [15] and double [2, 12] QWs have shown that both the magneto-transport and optical characteristics can deviate from the anticipated behaviour as charge is redistributed between subbands. Clearly an appropriate consideration of the wavefunction de-localization must be formulated for CDQWs in which the stability (off resonance) and even the absence (on resonance) of QH states could be an artifact of the density of states' (DoS's) quantization in a coupled 2DEG system.

Secondly, and of possible import to the proposed phase transition, is the destruction of the $\nu = 1$ state due to LL broadening. It has been proposed by many authors [16–18] that the width of the LLs increases with increasing magnetic field. Since the symmetric and anti-symmetric LLs are separated by a field independent gap ($\Delta_{SAS}$), see figure 1, it is conceivable that with an increasing field the tunnelling gap is smeared out, thereby suppressing the odd QH states.

The following work examines a range of coupled devices both on and off resonance. The presence of anomalous QH features at $\nu = N_{total}h/eB_{\perp}$ is shown to be a product of the tunnelling energy $\Delta_{SAS}$ and readily modelled in a fully self-consistent Poisson/Schrödinger solver: a model that does not include inter-layer interactions. Furthermore, an alternative mechanism, arising from the field dependent LL width, is proposed that could account for the absence of odd WH states in a CDQW.

## 2. Experimental data

Measurements were performed on GaAs/AlGaAs double quantum well (DQW) heterostructures grown by molecular beam epitaxy (MBE) upon (100) GaAs substrates. Electrons are confined to two GaAs quantum wells (QWs) of 150 Å width separated by a barrier layer of either $Al_{0.33}Ga_{0.67}As$ or AlAs. Carriers are supplied by modulation-doped AlGaAs layers situated above and below the two wells. Optical lithography and wet etching were used to define a Hall bar mesa and AuGeNi contacts were made that penetrated both 2DEGs. A surface Schottky front-gate enabled the density of the 2DEGs to be controlled. The growth characteristics for the three samples used are shown in table 1, together with their calculated coupling energies $\Delta_{SAS}$. Device T239 had an AlAs barrier, thus the barrier height is 1050 meV compared with 270 meV in T224/T225. As a result, the coupling energy is reduced whilst maintaining the same separation between 2DEGs.

**Table 1.** Growth parameters of the samples used including their mobilities and densities without illumination and at $V_{fg} = 0$ V. All QWs are 150 Å wide.

| Sample | Barrier (Å) | $N_{top}$ ($10^{15}$m$^{-2}$) | $N_{bottom}$ ($10^{15}$m$^{-2}$) | $\mu_{top}$ (m$^2$ V$^{-1}$ s$^{-1}$) | $\mu_{bottom}$ (m$^2$ V$^{-1}$ s$^{-1}$) | $\Delta_{SAS}$ |
|---|---|---|---|---|---|---|
| T225 | 300 | 1.3 | 1.3 | 105 | 116 | 0.36 $\mu$eV |
| T224 | 25 | 1.14 | 1.08 | 66 | 79 | 1.3 meV |
| T239 | 25 | 1.33 | 1.33 | 105 | 116 | 0.51 meV |

Experimentally, we measured both the longitudinal resistance ($R_{xx}$) and the Hall resistance ($R_H$) of the devices as a function of the front-gate bias ($V_{fg}$) for different applied fields. Where independent control of both the in-plane and perpendicular field components are necessary the sample has been mounted on an *in situ* rotating probe. Controlled field application coupled with computational control of the sample angle to the applied field (within $<0.1^{\circ}$) allows gate-sweeps at any combination of in-plane/perpendicular field (within the magnet's range) [28].

### *2.1. Uncoupled 2DEGs*

The formation and occupation of LLs with magnetic field remains similar to the single 2DEG when considering two un-coupled 2DEGs. However, the picture is complicated somewhat by the presence of a second layer. As expected, the layers are populated sequentially by the front-gate bias, starting with the 2DEG farthest from the gate. Once the gate begins to populate the top layer the lower 2DEG's carrier density ($N_{bottom}$) remains approximately constant. As the top 2DEG's screening is not perfect, the finite compressibility of the upper 2DEG ($\kappa_T$) determines the small density changes in the lower. Since the magnitude and sign of $\kappa_T$ varied with $N_{top}$ then $N_{bottom}$ also changes with gate bias. Therefore, the LL features associated with the lower 2DEG, especially at high fields, do not remain at fixed fields as the gate bias is altered. This is more pronounced in the narrow barrier devices considered within later sections.

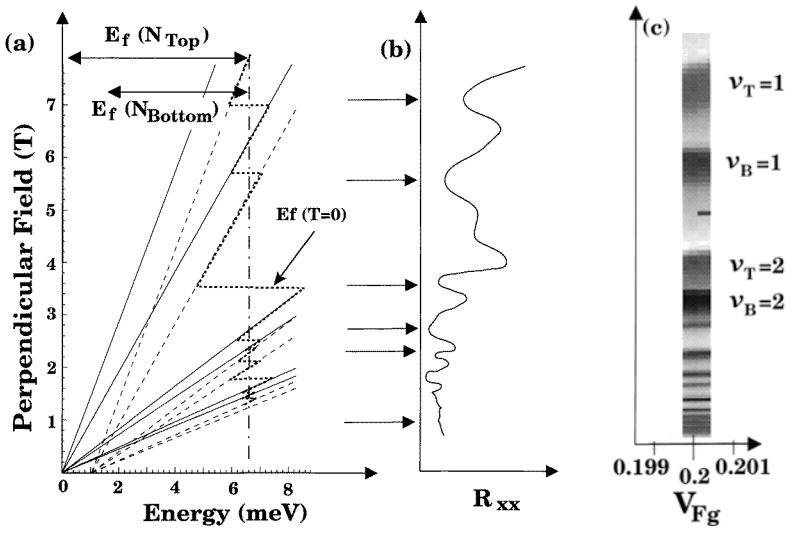


**Figure 2.** At $B_\perp = 0$ T and fixed front-gate bias, the 2DEG carrier densities are $N_{top}$ and $N_{bottom}$ for the top and bottom layers with Fermi energies $E_f(N)$. Upon applying a field (a) LLs are formed and the Fermi energy, shown by the dashed line, oscillates. (b) The corresponding longitudinal resistance oscillations. (c) The longitudinal resistance converted into a grey-scale in which light/dark regions indicate high/low resistances respectively.

Figure 2 shows the LL energies for both the top (solid lines) and bottom (dotted lines) 2DEGs at a fixed front-gate bias of +0.2 V in sample T225. As the magnetic field is swept the Fermi energy oscillates, figure 2(a), not just through one set of LLs but through two. In the absence of inter-well tunnelling, the 2DEGs remain localized within their respective QWs and the formation of LLs in one 2DEG has no effect upon the second. Strictly, the interlayer capacitance results in a degree of charge transfer between the two 2DEGs, however Davis *et al* [2] demonstrated that this effect does not significantly modify the notion of two independent LL ladders. Therefore, features are seen in the resistance, figures 2(b) and (c), that correspond to the de-population of LLs in either 2DEG.

The characteristics of an un-coupled DQW are clearly seen in figure 3, in which the full grey-scaled data set for sample T225 is shown. To create this grey scale, the four-terminal longitudinal resistance has been measured as a function of gate bias at different magnetic fields. The data within figure 3 may be divided into two section, (i) $V_{fg} < -0.5$ V and (ii) $V_{fg} > -0.5$ V.

At large negative gate biases ($V_{fg} < -0.5$ V) the 2DEG closest to the gate (top) has been fully depleted and one sees the field/bias LL fan of a single (bottom) 2DEG originating from the point $B_\perp = 0$ T, $V_{fg} = -0.85$ V.

For biases $V_{fg} > -0.5$ V, the top 2DEG is occupied, the top 2DEG's LLs fanning outwards from the origin at $B_\perp = 0$ T, $V_{fg} = -0.5$ V. Once both layers are occupied, one may identify the de-population of LLs in both of the 2DEGs for all fields/biases. Filling factors $\nu_B$ ($\nu_T$) associated with the bottom (top) 2DEGs are labelled by white (black) lettering on a black (grey) background.

Where the two LL fans intersect, pronounced resistance minima are observed. Minima that correspond to both layers occupying an integer number of filled LLs are assigned a filling index ($\nu_{total}$) corresponding to the total density, $N_{total} = N_{top} + N_{bottom}$. These intersections are marked by filled circles and labelled as $\nu_{total}(\nu_B, \nu_T)$.

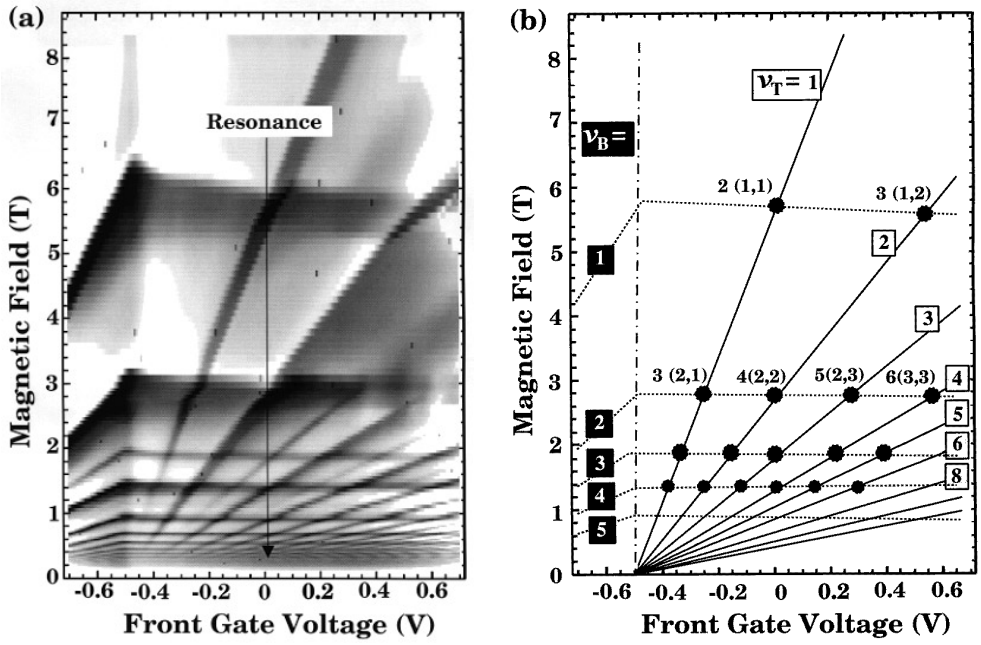


**Figure 3.** Longitudinal resistance of two uncoupled 2DEGs (T225) as a function of gate bias and perpendicular field. (a) The data are presented as a grey scale in which light/dark regions indicate high/low resistances respectively. (b) The filling factors ($\nu$) of the features seen in the grey-scaled data. The highlighted area shows the region of single 2DEG occupancy.

As there is no inter-layer tunnelling, the two 2DEGs have equal densities at resonance $V_{fg} = 0.05$ V. As the magnetic field is swept the Fermi energy jumps between doubly degenerate LLs, consisting of two LLs of the same LL index each associated with a 2DEG. Pronounced resistance minima are seen at even total filling factors ($\nu_{total} = 2, 4, 6, \ldots$), corresponding to $\nu_T = \nu_B = 1, 2, 3, \ldots$ in each layer.

### *2.2. High degree of coupling: T224*

The high degree of inter-layer tunnelling within sample T224 is reflected in the subband density/bias relationship (figure 4). Fast Fourier transforms (FFTs) of field sweeps from 0 to 1.5 T have been used to determine the subband densities at different gate biases. To resolve the SdH oscillations at low magnetic fields, the sample temperature was reduced to 320 mK.

A large subband anti-crossing is seen about resonance, $V_{fg} = 0$ V, indicating a high degree of wave-function hybridization. The experimental data are compared with the result of the self-consistent Schrödinger–Poisson model (dashed line) and excellent agreement seen.

Employing the same experimental technique as applied to samples T225 and T246, the longitudinal resistance has been obtained as a function of gate bias and magnetic field. Although the sample temperature has been reduced to 320 mK, the same characteristics are seen at 1.5 K [1]. Filling factors ($\nu_1$) associated with the first coupled subband are labelled by white lettering on a black background. Comparing the resistance grey-scale, figure 5, obtained for T224 with that of the lower $\Delta_{SAS}$ device (T225), figure 3, a number of significant differences are observed.

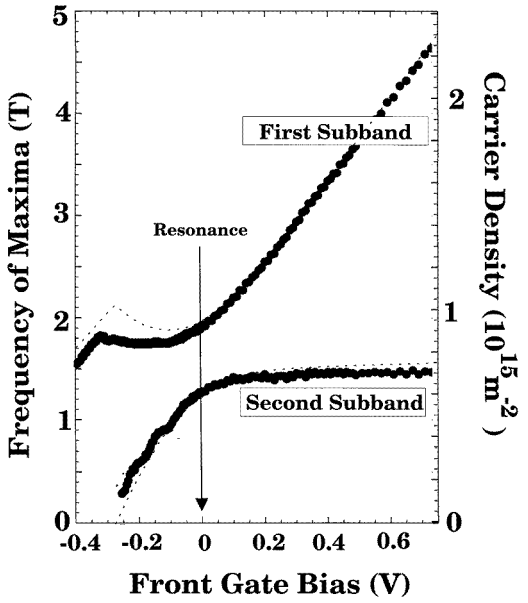


**Figure 4.** Sample T224's subband densities determined from experimental data (●) and from the self-consistent model with the LDA (dashed line).

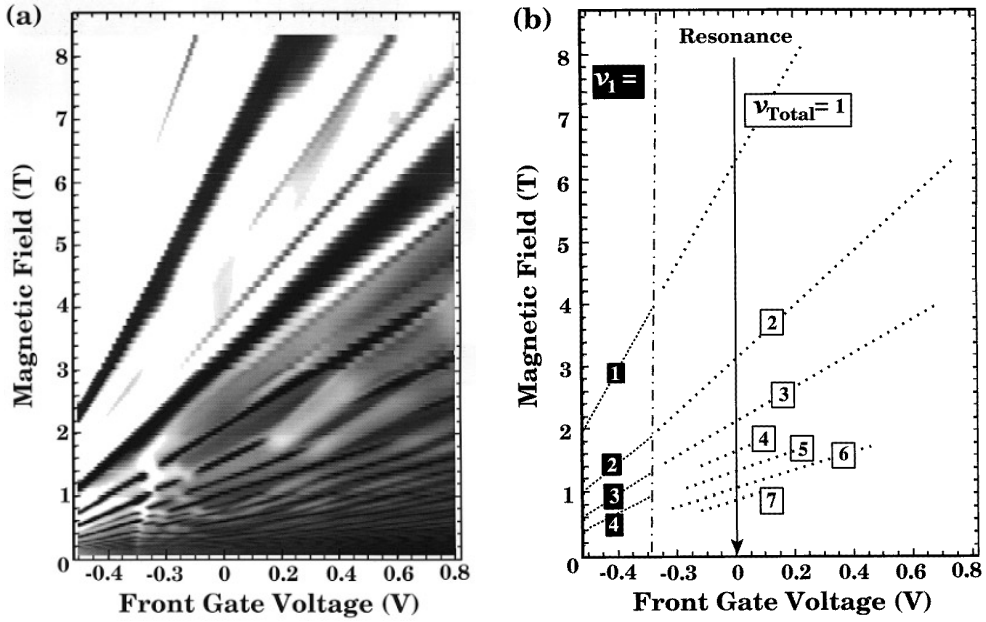


**Figure 5.** Longitudinal resistance of sample T224 as a function of gate bias and perpendicular field. (a) The data are presented as a grey scale in which light/dark regions indicate high/low resistances respectively. (b) The filling factors $\nu$ of the features seen with a single 2DEG occupied and at resonance. The sample temperature is 320 mK.

The strongest deviation is seen in the integer Hall states at $\nu_{total} = 1$ and 2. These states are continuous from large negative biases, where only a single subband is occupied, through the

bias regime where two subbands should be occupied. For the higher odd and even index filling fractions, there is a continuity of the pronounced resistance minima, nominally associated with intersections of two LL fans, through the point of resonance ($V_{fg} \approx 0$ V). This is observed for a range of intermediate fields between approximately 3 and 0.7 T. At lower fields (on resonance), and at slightly higher fields away from resonance, LLs may be identified with the occupation of two subbands; as evidenced by the presence of two FFT periods in the SdH data (figure 4).

As first mentioned within the introduction, both odd and even QH states should be seen at resonance as the subband densities remain significantly different. However, one should see *fainter* resistance features associated with the carrier density in each subband not strong resistance minima at filling factors corresponding to $\nu_{total}$ [1].

As discussed in detail by Davis *et al* [2], this observation can be assigned to the 'locking' of subbands at the chemical potential as the magnetic field is increased, a mechanism which is briefly outlined in the following.

In order that the total carrier density remain constant as the field is increased, the conduction band edge is either raised or lowered in energy as the chemical potential becomes 'pinned' at the 2DEG's LLs. In the absence of tunnelling the two 2DEGs/QWs are isolated from one another and, as the magnetic field is increased, changes in each of the 2DEGs' DoS/band profiles remain independent. However, in a CDQW, the wave-functions are delocalized and occupy the same space. Upon applying the magnetic field to a CDQW the pinning of an LL associated with one subband at the chemical potential will, therefore, affect the second subband. The results of self-consistent calculations [2] indicate that it is the *total* density within the CDQW that determines the filling factors seen. Therefore a 'continuity' of the $\nu_{total}$ QH states should be observed from either side of resonance across the 'matched' point. In such a case, the CDQW's characteristics resemble that of a *single* 2DEG rather than two parallel conducting, independent, subbands.

The experimental $\nu = 1$ and 2 QH features that we observe are, at first glance, anomalous with respect to this model in that they are seen not only at resonance, but over the full front-gate bias range. From the calculations of Davis *et al* [2] the 'locking' phenomenon has been shown to be dominant at resonance where the highest degree of wave-function hybridization occurs and away from resonance the characteristics of two weakly un-coupled/coupled 2DEGs were observed. However, with a sufficiently high degree of coupling the inter-layer tunnelling may be sufficient to lock the subbands together over a wide bias/field range, and the full bias range.

Alternatively, the anomalous QH states could be a related to the close proximity of the two electron gases and the $\nu = 1$ and $\nu = 2$ QH states may be stabilized by inter-layer correlations once the two 2DEGs are taken from resonance [10, 11].

### *2.3. Reduced coupling: T239*

To differentiate between an origin in either inter-layer correlations or coupling due to tunnelling, a wafer with a 25 Å AlAs barrier has been studied. Using an AlAs barrier, the inter-layer tunnelling is reduced whilst maintaining the same 2DEG–2DEG separation ($d$) as sample T224, therefore the inter-layer Coulomb energy is also approximately the same.

If inter-layer correlations were the origin of the anomalous $\nu = 1$ and 2 QH states then the same grey-scale characteristics would be seen in this sample as in the coupled sample T224; decreasing the inter-layer tunnelling should have *no* effect upon the sample characteristics. Conversely, if the anomalous QH states are a result of the de-localized wave-functions, decreasing the inter-layer tunnelling should significantly affect the magneto-transport data. Rather than observing anomalous QH states, the characteristics of a lower $\Delta_{SAS}$ sample, T225 for example, would be seen.

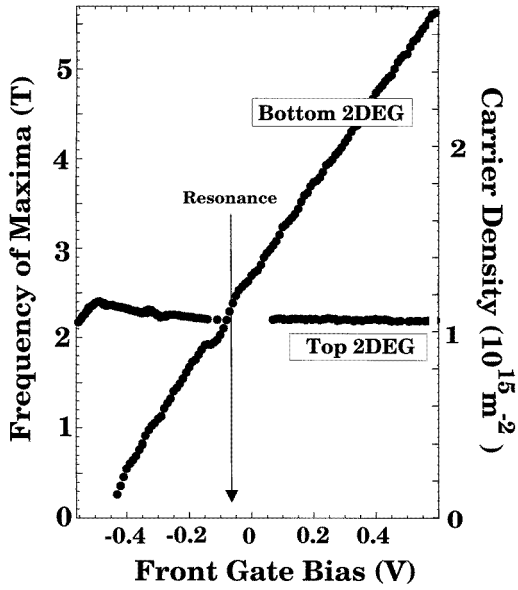


**Figure 6.** The subband carrier densities for sample T239 as determined from SdH oscillations at 0.32 K.

As in the previous section the low field (0.3 T $< B <$ 1.5 T) SdH data have been used to determine the subband densities (figure 6). In contrast to the comparable data set for sample T224 (figure 4), the subband anti-crossing is unresolved in the density–bias plot. Although this is partially due to the poor resolution of the FFT technique near resonance, the data clearly illustrate that the tunnelling is significantly less than in T224. From the self-consistent model the coupling energy (table 1) is 2.5 times smaller than that of T224, and the subband density difference at resonance is scaled equivalently: $\approx 0.2 \times 10^{15}$ m$^{-2}$ in T239.

The longitudinal resistance for sample T239 is shown as a function of bias and field in figure 7. Filling factors $\nu_1$ ($\nu_2$) associated with the first (second) subbands are labelled by white (black) lettering on a black (grey) background; intersections are marked by filled circles and labelled as $\nu_{total}(\nu_1, \nu_2)$.

This device shows *all* of the characteristics of the uncoupled sample T225: (i) at resonance $V_{fg} = -0.1$ V, only even filling indices ($\nu_{total}$) are clearly seen; (ii) a LL fan can be identified with each of the 2DEGs and the $\nu = 2$ QH state is no longer continuous across the full grey scale. As the carrier densities in T239 are slightly higher than in T224, equivalent LL intersections occur at higher magnetic fields. Although the $\nu = 1$ state within the bottom QW, $V_{fg} < -0.5$ V, is still present for a range of biases past $-0.5$ V, the cause of which is most probably the presence of some tunnelling in this sample, the strength of this resistance minimum decreases rapidly and at higher fields than those shown this feature does not extend across the entire bias range.

Despite the carrier density difference between T239 and T224, the data support a conclusion that the anomalous QH characteristics seen in the strongly coupled sample T224 are due to inter-layer tunnelling and are not states stabilized by inter-layer correlations. The observations upon the coupled 2DEG devices are summarized as follows. (i) At resonance, the field/bias characteristics of the QH states in T224 correspond to the *total* density, not the carrier densities of two 'mismatched' subbands. This indicates the onset of subband 'locking'.

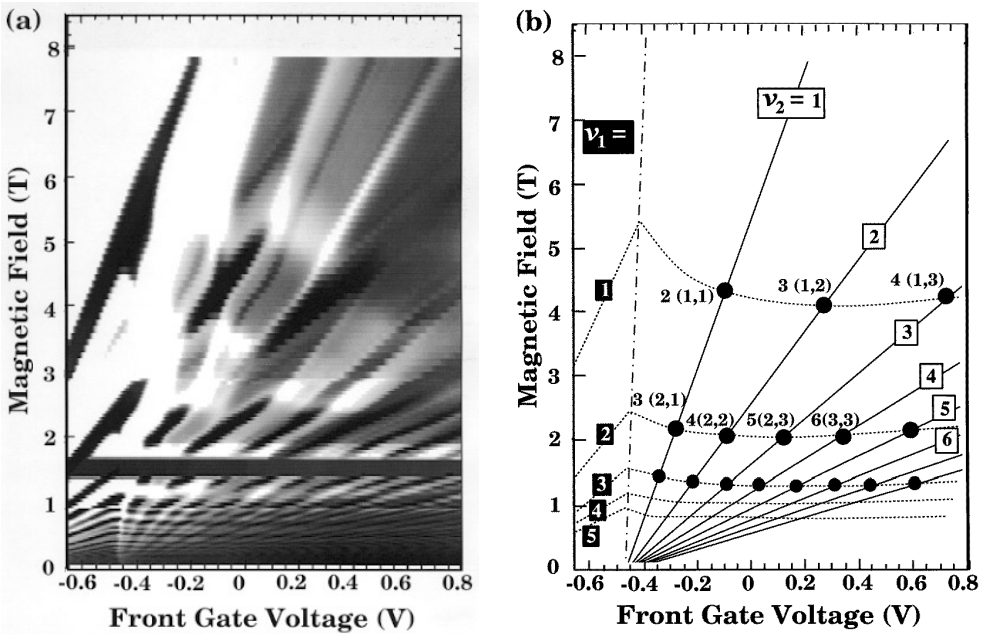


**Figure 7.** Longitudinal resistance of two strongly coupled 2DEGs (T239) measured as a function of gate bias for different perpendicular fields. (a) The data is presented as a grey scale in which light/dark regions indicate high/low resistances respectively. (b) The filling factors $\nu$ of the features seen in the grey-scaled data. The sample temperature was 0.32 K. The black, horizontal, feature seen at ≈1.5 T is due to missing data sweeps.

(ii) In the strongly coupled device, the $\nu = 1$ and 2 features are continuous for *all* gate biases and fields. (iii) Off resonance, the strongly coupled device shows LL filling fractions ($\nu > 2$) characteristic of weaker coupled devices. (iv) At resonance, only even index filling fractions are seen in the AlAs barrier sample T239 and no anomalous QH states are present.

The results from sample T239 indicate that inter-layer tunnelling, not inter-layer correlations, are responsible for the anomalous $\nu = 1$ and 2 features. This conclusion can be supported through the application of a strong in-plane field upon sample T224.

### *2.4. In-plane field dependence: T224*

By applying an in-plane field component, the Fermi surfaces (FSs) associated with each 2DEG are moved apart in momentum space. Small in-plane fields change the subband densities [20], whilst an in-plane and perpendicular field component result in magnetic breakdown [21]. The application of a very large in-plane field totally removes the Fermi surfaces from one another, prohibiting inter-well tunnelling. In order to fully separate the FSs of two 2DEGs with carrier densities of $\approx 0.9 \times 10^{15}$ m$^{-2}$ separated by 175 Å, an in-plane field in excess of 6 T is required.

Figure 8 illustrates the effect of a 10 T in-plane field upon sample T224. This in-plane field is sufficient to separate the FSs in sample T224 for the full gate bias range considered. Filling factors $\nu_1$ ($\nu_2$) associated with the first (second) subbands are labelled by white (black) lettering on a black (grey) background, intersections are marked by filled circles and labelled as $\nu_{total}(\nu_1, \nu_2)$.

Only the even integer Hall states are seen at resonance, $V_{fg} = 0$ V. This is characteristic of the samples with no inter-layer tunnelling, as illustrated in figure 3. Further, there are no

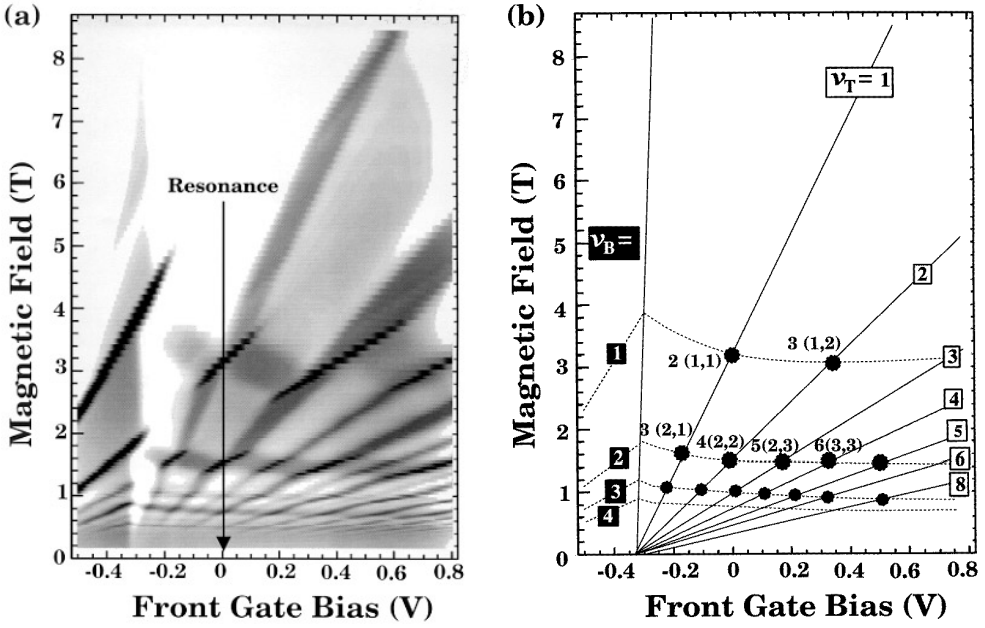


**Figure 8.** The longitudinal resistance as a function of gate bias and perpendicular fields. (a) The results are presented as a grey scale in which light/dark regions indicate high/low resistances respectively. (b) The filling factors $\nu$ of the features seen in the grey-scaled data. The measurements are made with a *constant* in-plane field component of 10 T at 1.5 K.

signs of any anomalous $\nu = 1$ and 2 resistance minima (figure 5) either on or off resonance: the transport characteristics now duplicate, albeit at lower fields, the results for an uncoupled device (i.e. sample T225). Therefore, we conclude that the anomalous QH features seen at $\nu = 1$ and 2 are a result of inter-layer tunnelling, in agreement with the data from T239 where the coupling was modified by increasing the inter-layer barrier.

## 3. Theoretical model

Although other authors have invoked inter-layer correlations to explain the stability of the $\nu = 1$ state off resonance [10, 11], the data presented demonstrate that the stability is not due to inter-layer interactions: one must first consider the affect of the DoS's quantization in a coupled system. For CDQWs [2], the single–double layer transition is shown to be a result of wave-function hybridization and can be modelled with a self-consistent Schrödinger–Poisson solver. No inter-layer correlations are included within this model though intra-layer correlations are accounted for through the LDA. The model assumes zero temperatures, with the LL broadening accounting for scattering/thermal disorder.

The Landau levels are given a width through a field dependent Gaussian function and the density of states of the $i$th subband $D(E)_i$ is given by [22, 23]

$$D(E)_i = \frac{m^*}{\pi\hbar^2} \sum_L \sum_s \frac{1}{\Gamma(LL)_i\sqrt{B}} \exp\left[-2\left(\frac{(E - E_i)}{\Gamma(LL_i\sqrt{B}}\right)^2\right]. \tag{1}$$

In equation (1), $L = 0, 1, 2, \ldots$ and $s = -\frac{1}{2}, +\frac{1}{2}$ are the Landau level and spin indices respectively and $\Gamma(LL)_i$ is the Gaussian width at $B = 1$ T (taken to e 0.1 meV). A background

of states has not been included, therefore the DoS becomes zero between sufficiently narrow LLs. The carrier density in each subband $N_i$, is given by the integral in equation (2):

$$N_i = \int_{-\infty}^{\infty} D(E)_i \, \mathrm{d}E. \tag{2}$$

The resistance calculations presented are performed using either of two phenomenological relations. The theoretical data shown in section 3.2 uses a standard phenomenological relation given by equation (3). Here the states contributing to the conductance are modelled by a Gaussian function with a width $\Gamma_i$. The Landau level energies $E_{i,L}(B)$ incorporate the spin splitting and are given by $(E_{i,L}(B) = E_i + (L + \frac{1}{2})\overline{h}\omega_c + sg^*\mu_B B)$

$$\sigma_{xx}(i) = \frac{e^2}{h} \sum_L (L + \tfrac{1}{2}) \exp\left[-2\left(\frac{E_f - E_{(i,L)}(B)}{\Gamma_i\sqrt{B}}\right)^2\right]. \tag{3}$$

The transverse conductivity $(\sigma_{xy}(i) = -eN_i/B)$ and longitudinal conductivity are used to calculate the resistivity through the tensor relation $(\rho = \sigma^{-1})$ for parallel conducting layers.

It was found that, in order to obtain qualitative agreement with the grey-scaled experimental data, a second phenomenological relation $(\sigma_{xx}(i) = \sigma_{itotal} - \sigma_{ilocalized})$ was employed. In these calculations, section 3.1, $\sigma_{itotal}$ (equation 4) is the total contribution to the conductance from all of the LLs lying below the Fermi energy and $\sigma_{ilocalized}$ (equation (5)) is a Gaussian distribution of states, centred between the LLs, which do not contribute to the conductance. This relation is aimed at reproducing the high field behaviour $(\nu < 2)$ and is based solely upon its ability to duplicate the experimental results under the requirement that both even and odd IQH states have resistance minima of similar widths at all fields:

$$\sigma_{i\,total} = \frac{e^2}{h}\left(\frac{E_f - E_i}{\overline{h}\omega_c}\right) \qquad (E_f > E_i) \tag{4}$$

$$\sigma_{i\,localized} = \frac{e^2}{h} \sum_{L'} \left(\frac{L'}{2} + \frac{1}{2}\right) \exp\left[-2\left(\frac{E_f - E_{(i,L')}(B)}{\Gamma_i\sqrt{B}}\right)^2\right]. \tag{5}$$

Here $i$ is the subband identifier and $L' = 0, 1, 2, \ldots$ is a Landau level counter, $N_i$ is the $i$th subband density and $\Gamma_i$ the energy width of the non-contributing states. The energy $E_{(i,L')}(B)$ of points midway between conducting LLs is given by $E_{(i,L')}(B) = (L'/2 + \frac{1}{2})\overline{h}\omega_c$.

In both cases the transverse conductivity $(\sigma_{xy}(i) = -eN_i/B)$ and longitudinal conductivity are used to calculate the resistivity through the tensor relation $(\rho = \sigma^{-1})$ for parallel conducting layers.

### *3.1. Model: anomalous $\nu = 1, 2$ QH states*

The model results for the coupled device, T224, are shown in figure 9. The calculations for T224, although not in complete agreement with the experiment, do duplicate the major features at high fields due to subband locking. As a number of approximations, including the Gaussian form of the DoS, the form of the conductance calculation, $g^*$ factors and so forth, have been made, complete agreement is not expected.

The important result arising from the model is that a strong $\nu_{total} = 1$ state is observed to be continuous across the entire field/bias range, although only a weaker $\nu_{total} = 2$ state is seen. That these continuous states are seen at all in a model with no inter-layer correlations is conclusive evidence that they are a result of the wave-function hybridization in strongly coupled 2DEGs.

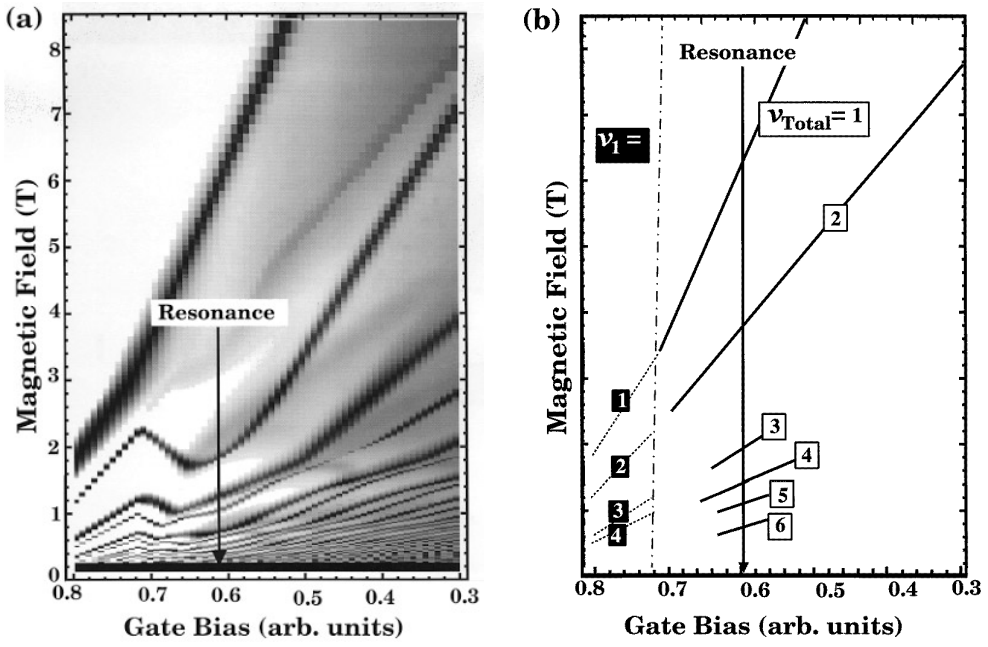


**Figure 9.** The longitudinal resistance calculated for sample T224 as a function of gate bias and perpendicular field. (a) The results are presented as a grey scale in which light (dark) regions indicate high (low) resistances respectively. (b) The filling factors $\nu$ of the features seen with a single subband occupied and at resonance.

### *3.2. Model: Landau level broadening*

It must be noted that in order to construct the proposed phase boundaries [9] the mixing of LLs originating from different subbands has been neglected. Nominally, if the coupling gap can be resolved at zero (low) magnetic fields, one would also expect to fully resolve the gap at high magnetic fields. However, a 2DEG's DoS in a field can be described by a series of Gaussian functions which increase in width with field [22, 23]. At a sufficiently high field the odd index LLs (e.g. the $\nu = 1$ LLs in each subband) separated by a field independent gap $\Delta_{SAS}$ begin to mix, thereby suppressing the tunnelling gap. To account for the LL width, we use the theoretical self-consistent model to construct a comparable 'phase' diagram that describes the stability of the $\nu_{total} = 1$ state at resonance.

Devices with fixed QW widths of 150 Å and differing barrier widths have been modelled. A front- and back-gate bias was used to vary the total density in the CDQW whilst maintaining resonance. The magnetic field at which a QH state at $\nu_{total} = 1$ should occur is calculated from the subband densities. The $g$-factor remains constant with a value of 3.1 and to account for the LL broadening the LLs are defined by a width $\Gamma_{LL}\sqrt{B}$ (see equation (1)).

A typical set of resistance calculations is illustrated in figure 10 for a 30 Å barrier CDQW with different total carrier densities. The data clearly show that the $\nu_{total} = 1$ state is suppressed as the total carrier density is increased. The higher odd $\nu$s remain pronounced (though slightly diminished) once the $\nu = 1$ state has disappeared, indicating that higher magnetic fields would be required to suppress these states.

The charge density distributions (figure 10) for three selected $\nu = 1$ states illustrate the aforementioned suppression of the tunnelling gap as the LL width increases. It is clearly seen

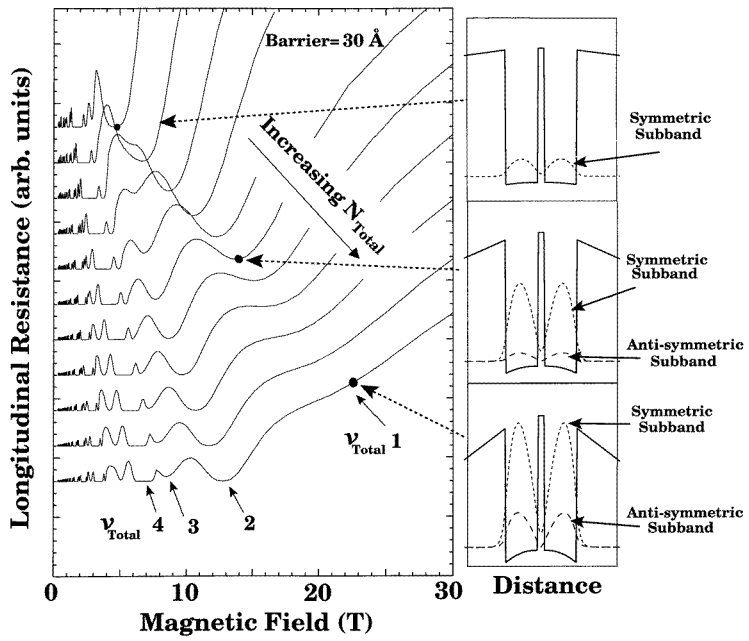


**Figure 10.** The longitudinal resistance calculated using the self-consistent model for a single device with a 30 Å barrier. The total density varies from 1.6 to $6.6\times10^{15}$ m$^{-2}$. Also shown are the subband charge distributions calculated at $\nu = 1$ with three different $N_{total}$.

that as the field at which the $\nu = 1$ state occurs is increased, carriers then begin to populate the anti-symmetric $\nu = 1$ LL.

It is also observed that the $\nu = 2$ state is present in both the lowest and highest $N_{total}$ resistance traces and is strongly suppressed at intermediate densities. This may be readily ascribed to the system crossing between the two limits $g^*\mu_B B <> \Delta_{SAS}$. As the charge excitation gap for the $\nu = 2$ state is given by $|g^*\mu_B B - \Delta_{SAS}|$, this state vanishes when the Zeeman and tunnelling energies are comparable.

## 4. Discussion

To consider the experimental data in the light of the many-body interaction induced 'bi-layer phase transition' in CDQWs, three energy scales are relevant: the inter-well, single particle, tunnelling gap $\Delta_{SAS}$, the inter-layer energy $e^2/(4\pi\epsilon_0\epsilon_r d)$ and the intra-layer Coulomb energy $U$, $e^2/(4\pi\epsilon_0\epsilon_r l_B)$. Here $l_B$ is the magnetic length and $d$ the inter-layer separation.

Our experimental odd ($\nu_{total}$) QH states are plotted on the phase diagram of (intra-/inter-layer energies $= d/l_B$) and ($\Delta_{SAS}$/intra-layer energy, figure 11. The filling factor corresponds to the total DQW's density, and the dashed lines indicate the proposed boundaries separating a region in which odd QH states should be seen and the bi-layer regime in which no odd QH states should be seen [9].

A similar phase diagram has been constructed using the theoretical model calculations. The tunnelling gap $\Delta_{SAS}$ is determined for each data point and the layer separation $d$ is taken to be the centre–centre distance between the QWs. To collate a large number of fields/samples, the phase diagram shown in figure 12 is constructed by adding points corresponding to the

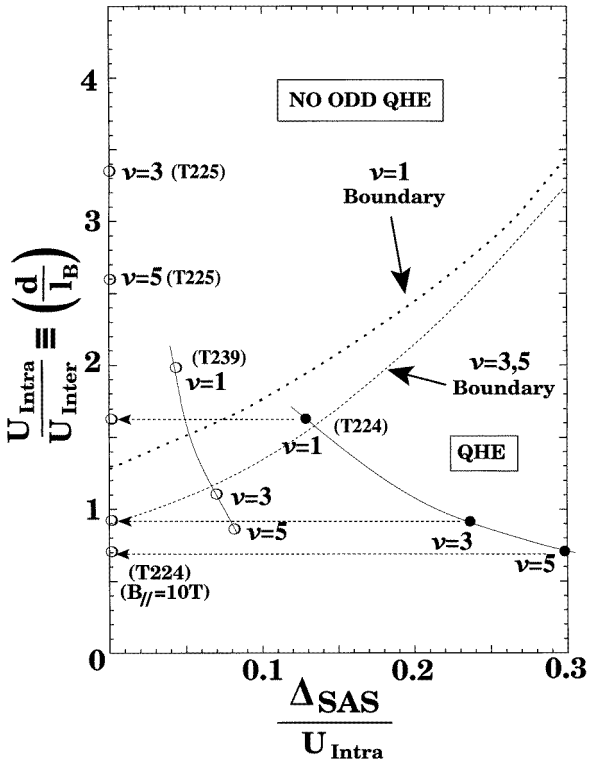


**Figure 11.** Phase diagram for bi-layer transition with experimental data points for samples T224, T224 (at $B_{\|} = 10$ T), T239 and T225. A complete, solid circle (●) indicates a strong observable QH state whilst an empty circle (○) no QH state.

presence (solid fill) or absence (white fill) of a $\nu_{total} = 1$ QH state in the calculated longitudinal resistance. Partially suppressed states are indicated by a partially filled point.

As the tunnelling energy does not change significantly with the CDQW's total density, the solid lines that link data points for any given sample follow a line of approximately constant $\Delta_{SAS}$ and changing magnetic field: moving to higher $d/l_B$, the total density/magnetic field at which $\nu_{total} = 1$ occurs increases. The data in figure 10 are one such data set, which maps out the data points for the 30 Å barrier device.

Based upon the data within figures 10 and 12, there exists a critical boundary defined by a coupling energy ($\Delta^*_{SAS} \approx 0.14\sqrt{B}$ meV) beyond which the $\nu_{total} = 1$ state is no longer stabilized by the inter-layer tunnelling. This critical limit corresponds to when $\Delta_{SAS}$ becomes comparable to the LL width of $0.1\sqrt{B}$ meV used within the simulation.

It should be noted that the model has been greatly simplified by assuming a Gaussian LL DoS and there exists a great deal of uncertainty regarding their correct form. The initial DoSs for a 2DEG in a strong magnetic field were proposed by Ando and Uemura [24], their results predicting an ellipsoidal lineshape with a width ($\Gamma$) of ($1.39\sqrt{B}/\mu$) meV. However these calculations only considered short range scattering and inter-LL coupling was neglected. It was also assumed that the zero-field mobility (scattering) remained unaffected by the applied field. Calculations by Das Sarma and Xie [25] illustrated that the inclusion of long range scattering and LL coupling effects modified the mobility in a field, increasing the LL width above that calculated by Ando and Uemura. Further theoretical studies have employed

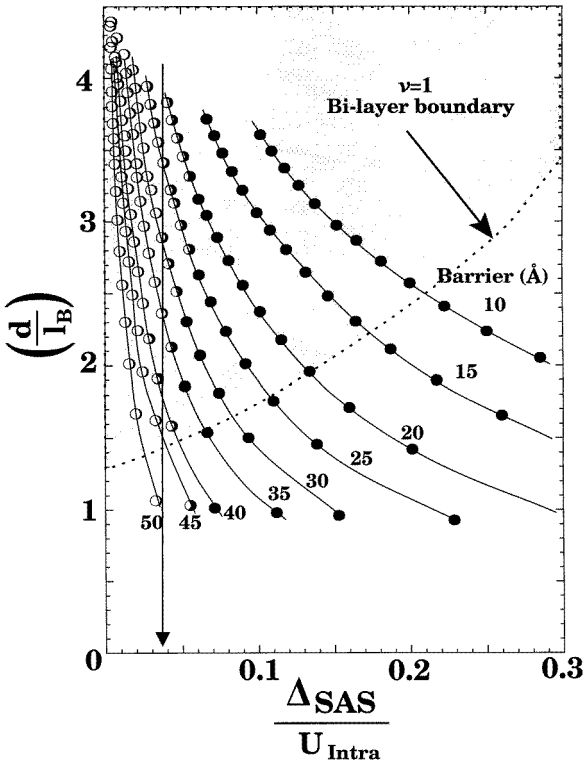


**Figure 12.** Phase diagram for the theoretically determined $\nu_{total} = 1$ data points. A complete, solid circle (●) indicates a strongly pronounced QH state whilst an empty circle (○) no QH state. Differing degrees of the QH minima strength are indicated by partially filled circles. The vertical arrow indicates the QHE/no QHE boundary from the simulation.

Gaussian lineshapes [18, 26] or lineshapes related to the topology of the 2DEG's confinement [25].

Experimental estimates of the DoS's form are also varied. Gaussian functions with a $\sqrt{B}$ dependent width have been reported with magneto-capacitance [23] and de Haas–van Alphen data [22], albeit with a larger width than in Ando's calculation. In contrast, Ashoori and Silsbee [27] have reported a good fit whilst employing Lorentzian functions with a field independent LL width.

The simplified conductance calculation includes further approximations such as a fixed $g$-factor, Gaussian function and a $\sqrt{B}$ dependence for the LL width (following the DoS broadening). However, for this work a more rigorous approach is not necessary and the current model has demonstrated that the magnitude of the LL broadening has a significant affect upon whether or not an IQH state is seen at $\nu = 1$. This leads to the important conclusion that it is incorrect to draw the phase diagrams neglecting the LL broadening as this clearly plays an important role in the observation of the $\nu = 1$ state.

Comparing the results of the self-consistent model with the experimental data, there is a degree of uncertainty in fitting the experiment to any transition boundary. There are errors in estimating the experimental tunnelling energies and, whereas $\Delta_{SAS}$ for T224 has been determined experimentally, the gap for T239 remained unresolved and the simulation value of 0.514 meV only provides an upper limit. Also, the layer separation is not strictly the

centre–centre distance as the wavefunctions do have a finite width in the confinement direction. Both of these increase the uncertainty in the experimental data's position in the phase diagram.

If the LL broadening were the cause of the suppressed odd QH states, the model's assumption that the LL width at 1 T remains 100 $\mu$ eV, irrespective of device, will be invalid. A rigorous calculation accounting for a field/device dependent $g$-factor and alternative forms for the DoS/conductance would be required to obtain full agreement with experiment.

## 5. Summary

The occurrence of IQH states in DQW systems has been investigated in a wide range of samples with varying degrees of tunnelling and with a high in-plane magnetic field. Upon applying a large perpendicular field the characteristics of a strongly coupled DQW resemble that of a single 2DEG. Further, anomalously strong QH states are observed that persist as the CDQW is taken off-resonance. The stability of the odd $\nu_{total} = 1$ and 2 IQH states with density imbalance from resonance is experimentally shown to be a result of the inter-layer tunnelling and not a product of inter-layer correlations.

Furthermore, theoretical modelling employing a self-consistent Schrödinger–Poisson solver duplicates the experimental observations. Calculations of the resistance and charge distributions in coupled/de-coupled systems show that subband locking [2] may occur, at high magnetic fields, irrespective of the density imbalance from resonance.

Using the self-consistent model, a phase diagram for the $\nu_{total} = 1$ tunnelling stabilized state (at resonance) has been constructed. The results show that the $\nu_{total} = 1$ QH state is only stabilized by inter-layer tunnelling for a specific range of $\Delta_{SAS}$ and magnetic fields.

It is by no means implied that the collapse of odd IQH states through many-body interactions does not occur. Rather, an alternative mechanism is proposed by which an equivalent experimental phenomenon may result. Whilst the magnetic field is small and $\Delta_{SAS}$ is large the finite field dependent width of the LLs does not significantly affect the CDQW and a $\nu_{total} = 1$ state is seen. However at higher fields, or lower $\Delta_{SAS}$, once the LL broadening and $\Delta_{SAS}$ become comparable the tunnelling gap is destroyed and the $\nu_{total} = 1$ state suppressed. This mechanism has, to date, not been considered in the literature despite the important consequences that LL broadening has upon current studies of CDQWs.

## Acknowledgments

This work was supported by the EPSRC. One of the authors, DAR, would like to acknowledge support from the Toshiba Cambridge Research Centre.

## References

[1] Millard S, Patel N K, Simmons M Y, Hamilton A R, Ritchie D A and Pepper M 1996 *J. Phys.: Condens. Matter* **8** 311
[2] Davis A G, Barnes C H W, Zolleis K R, Nicholls J T, Simmons M Y and Ritchie D A 1996 *Phys. Rev.* B **54** 17 331
[3] Song He, Xie X C, Das Sarma S and Zhang F C 1991 *Phys. Rev.* B **43** 9339
[4] Boebinger G S, Pfeiffer L N and West K W 1992 *Phys. Rev.* B **45** 11 391
[5] Suen Y W, Jo J, Santos M B, Engel L W, Hwang S W and Shayegan M 1991 *Phys. Rev.* B **44** 5947
[6] Suen Y W, Jo J, Santos M B, Engel L W and Shayegan M 1992 *Surf. Sci.* **263** 152
[7] Murphy S Q, Eisenstein J P, Boebinger G S, Pfeiffer L N and West K W 1994 *Phys. Rev. Lett.* **72** 728
[8] Hamilton A R, Simmons M Y, Bolton F M, Patel N K, Millard I S, Nicholls J T, Ritchie D A and Pepper M 1996 *Phys. Rev.* B **54** 5259

[9] MacDonald A H, Platzman P M and Boebinger G S 1990 *Phys. Rev. Lett.* **64** 1793
[10] Sawada A, Ezawa Z, Ohno H, Horikoshi Y, Sugie O, Kishimoto S, Matsukura F, Ohno Y and Yasumoto M 1997 *Solid State Commun.* **103** 447
[11] Sawada A, Ezawa Z F, Ohno H, Horikoshi Y, Kishimoto S, Matsukura F, Ohno Y, Yasumoto M and Urayama A 1998 *Physica* B **251** 836
[12] Zolleis K R, Barnes C H W, Davies A G, Simmons M Y, Ritchie D A and Pepper M 1998 *Physica* B **251** 850
[13] Kelly M J and Hamilton A 1991 *Semicond. Sci. Technol.* **6** 201
[14] Hayes D G, Skolnick M S, Whittaker D M, Simmonds P E, Taylor L L, Bass S J and Eaves L 1991 *Phys. Rev.* B **44** 3436
[15] Ensslin K, Sundaram M, Wixforth A, English J H and Gossard A C 1991 *Phys. Rev.* B **43** 9988
[16] Weiss D, Mosser V, Gudmundsson V, Gerhards R R and von Klitzing K 1987 *Solid State Commun.* **62** 89
[17] Ensslin K, Heitmann D, Gerhardts R R and Pllog K 1989 *Phys. Rev.* B **39** 12 993
[18] Gerhadts R R 1976 *Surf. Sci.* **58** 227
[19] Usher A 1995 *Phys. Rev.* B **75** 4293
[20] Boebinger G S, Passner A, Pfeiffer L N and West K W 1991 *Phys. Rev.* B **43** 12 673
Lyo S K 1994 *Phys. Rev.* B **50** 4965
Junwirth T and Smrćka L 1993 *J. Phys.: Condens. Matter* **5** L217
[21] Harff N E, Simmons J A, Lyo S K, Klem J F, Boebinger G S, Pfeiffer L N and West K W 1997 *Phys. Rev.* B **55** 13 405
[22] Eisenstein J P, Stormer H L, Narayanamurti V, Cho A Y, Gossard A C and Tu C 1985 *Phys. Rev. Lett.* **55** 875
[23] Smith T P III, Wang W I and Stiles P J 1986 *Phys. Rev.* B **34** 2995
[24] Ando T and Uemura Y 1974 *J. Phys. Soc. Japan* **36** 959
[25] Das Sarma S and Xie X C 1988 *Phys. Rev. Lett.* **64** 738
[26] Wegner F 1988 *Z. Phys.* **51** 279
[27] Ashoori R C and Silsbee R H 1992 *Solid State Commun.* **81** 821
[28] Millard I S, Patel N K, Foden C, Linfield E H, Ritchie D A, Jones G A C and Pepper M 1997 *J. Phys.: Condens. Matter* **9** 1079